Organic Compound/Metal Oxide Hybrid Thin Film Prepared by the Liquid Phase Deposition Method

Deki, Shigehito
Kodama, Yasuaki
Mizuhata, Minoru

(Citation)
ECS Transactions,16(25):73-83

(Issue Date)
2009

(Resource Type)
journal article

(Version)
Version of Record

ECS Transactions, 16 (25) 73-83 (2009)
10.1149/1.3115525 ©The Electrochemical Society

Organic Compound/Metal Oxide Hybrid Thin Film Prepared by the Liquid Phase Deposition Method

Shigehito Deki, Yasuaki Kodama, and Minoru Mizuhata*

* Department of Chemical Science and Engineering,
Graduate School of Engineering, Kobe University
1-1, Rokkodai, Nada, Kobe, 6578501, Japan

Organic compound/metal oxide composite thin films have been prepared by the liquid-phase deposition method in one-step deposition technique. Organic dyes were added to the metal fluoro-complexes aqueous solution in order to entrap these dyes within the growing thin films of metal oxides, yielding organic dye/metal oxide hybrid materials. According to Raman spectroscopy and X-ray photoelectron spectroscopy, the formation of the materials in the case of cationic dyes can be explained by electrostatic interaction between negative charge density at the fluorinated surface of metal oxides and the cationic dyes. UV-Vis results indicate that stilbazo and pyrocatechol violet (catecholate dye molecules) form a charge transfer complex with metal oxides through the catechol moiety with a bidentate linkage.

Introduction

Hybrid organic-inorganic materials have received growing attention over the past 10 years, in particular because they are attractive candidates for optical devices, catalysts, sensor coatings etc. (1). The most common method of preparation of these materials is the insertion of organic molecules into the galleries or inorganic lattices, including 3-D frameworks, 2-D layers host, 1-D tunnel hosts, etc. (2,3). In general, the synthesis of organic/inorganic hybrid materials is carried out in two or more successive steps including the preparation of metal oxide, surface modification due to the need of high temperature treatment, etc. (4,5).

We have recently developed and promoted a novel aqueous solution-based process to prepare metal oxide thin films, the so-called liquid phase deposition (LPD) method (6-9). The advantage of the LPD method is the ability to synthesize hybrid materials under an ambient condition without any post-annealing process. Based on this technique, organic/inorganic hybrid thin films such as alkyl sulfate and alkylbenzene sulfonate surfactants/TiO_2 hybrid films and protein-templated organic/inorganic hybrid materials have been developed (10,11). However, to-date, there are only a few investigation on the molecular structures of organic compound which can be incorporated into metal oxide films. The effect of molecular structures on the deposition rate of metal oxide has not yet been reported.

In this study, we have prepared organic dye/metal oxide hybrid thin films by LPD method, and investigated the structural properties of organic compound incorporated into metal oxide films. The synthesized materials have been characterized by Raman

spectroscopy, XPS, UV–vis spectroscopy, SEM and ICP-AES.

Experimental

Materials

Soda-lime glass was used as the substrate. H_3BO_3 and Al metal were employed as the F^-. scavenger. The following complex material were used as parent solutions: titanium oxide $\{(NH_4)_2TiF_6\}$, silicon oxide $\{(NH_4)_2SiF_6\}$, zirconium oxide $\{H_2ZrF_6\}$. The organic dyes consisted of: methylene blue (MB), neutral red (NR), rhodamine B (RB), Malachite green (MG), eosin Y (EY), stilbazo, pyrocatechol violet (PCV) and aluminon (Figure 1). Stilbazo and PCV are the catecholate dye molecules.

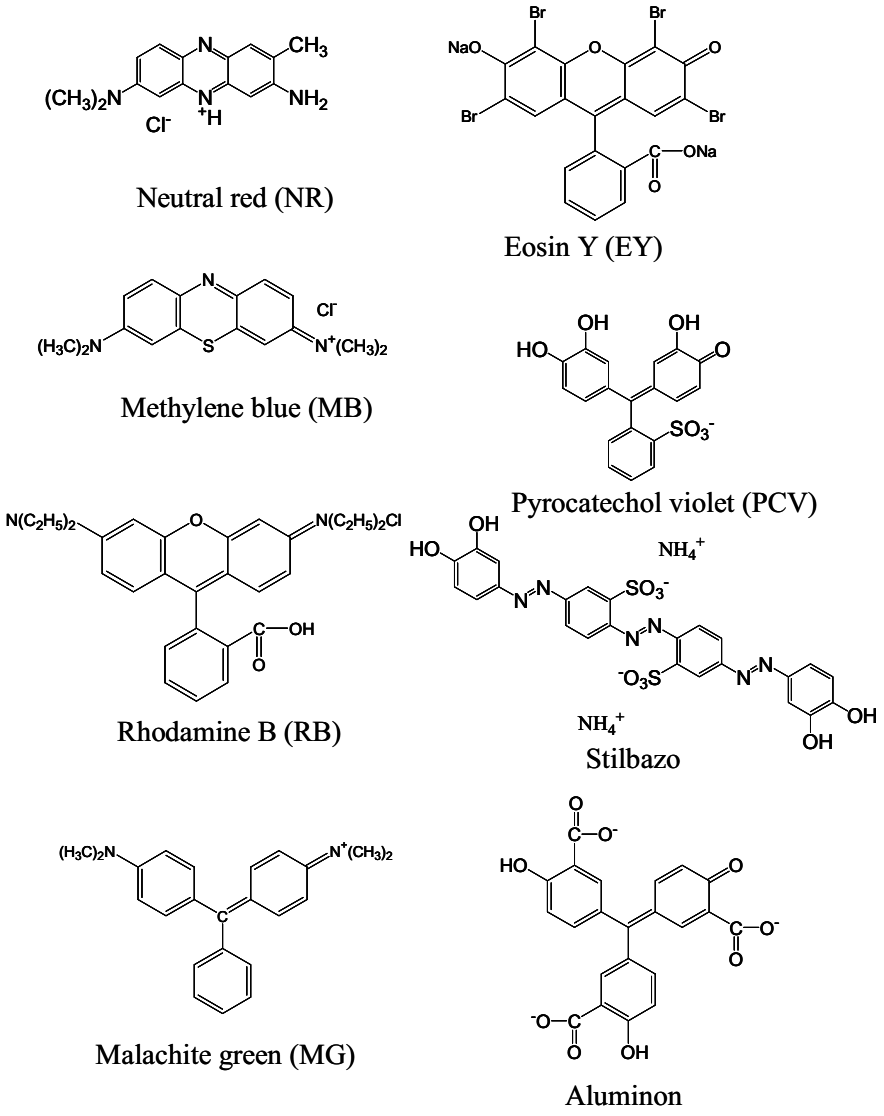

Figure 1. The structures of organic dyes.

Sample preparation

The deposition of organic dye/metal oxide composite thin film was carried out in one step as follows. The substrates were immersed into the treatment solution containing metal-fluoro complex, the F^- scavenger and organic dye aqueous solution. These solutions were mixed at various compositions and used as the treatment solution. For each system, the following composition was used: titanium oxide system, 10 mol/dm^3 [$(NH_4)_2TiF_6$] and 0.20 mol/dm^3 H_3BO_3; silicon oxide system, 0.10 mol/dm^3 [$(NH_4)_2SiF_6$] and 0.20 mol/dm^3 H_3BO_3; zirconium oxide system, 50 mmol/dm^3 [H_2ZrF_6] and 2 x 12 cm^{-2} Al metal. The organic dyes were dissolved in the treatment solution at a concentration of 0.0–1.0 mmol/dm^3.

After degreasing and washing ultrasonically, the substrates were immersed into the treatment solution and suspended therein vertically. The reaction varied from: 2-52 h and the temperature from: 30-60ºC. The substrates were then removed from the treatment solution, washed with distilled water and dried at ambient temperature.

Sample characterization

The optical transmission and scattering measurements of the thin films were performed using UV-Vis Spectrophotometer (JASCO V 7200). The surface morphologies of the films were observed by field emission scanning electron microscope (FE-SEM; JEOL JEM-6335F). In order to prevent the surface of samples from electron charging up, the samples were coated using carbon coater (40FM; Meiwa Shoji Co. Ltd.). The amount of chemical elements contained in the deposited films was measured by inductively coupled plasma atomic emission spectrometry (ICP-AES; HORIBA Ltd., ULTIMA 2000). The deposited films on a substrate were dissolved into 20 ml of 3.78 mol dm^{-3} HCl. The crystalline structures were investigated using X-ray diffractometer (Rigaku RINT-TTR/S2) equipped with a scintillation detector, and a rotating Cu anode operating radiation at 50 kV and 300 mA. Using parallel beam optics formed by a multilayered mirror (Rigaku, Cross Beam Optics attachment), asymmetric 2θ scans with a fixed small incident angle were carried out. Raman spectra were measured with Horiba T-64000 excited by 532 nm SHG of Nd-YVO4 laser. Infrared measurement were performed by means of FT-IR 615 type spectrophotometer (JASCO), coupled with a diffuse reflectance attachment DR-600B (JASCO). The resolution was 2 cm^{-1}. Chemical states of F comprising into the films were analyzed with X-ray photoelectron spectroscopy (XPS; JEOL JPS-9010MC) with AlKα as the X-ray source (1486.6 eV) and charge neutralizer. Calibration for spectra was performed by taking the C 1s electron peak (E_b = 284.6 eV) as internal reference.

Results and discussion

Incorporation of organic compound into metal oxide thin film

Using the LPD process, from each treatment solution containing organic dye, metal oxide thin film was deposited on the substrate. The deposited films were observed with naked eyes from which, two categories of samples could be distinguished as shown in Table 1: (*i*) the circle mark which indicate colored thin film, (*ii*) samples marked with

Table 1. Organic dye – metal oxide composite thin film.

	MB	NR	RB	MG	EY	Stilbazo	PCV	Aluminon
TiO_2 system	○	○	×	×	×	○	○	○
SiO_2 system	○	○	○	○	×	×	×	×
ZrO_2 system	○	○	×	×	×	○	○	

○ ; Organic dye/metal oxide composite thin film
× ; non deposition or no colored

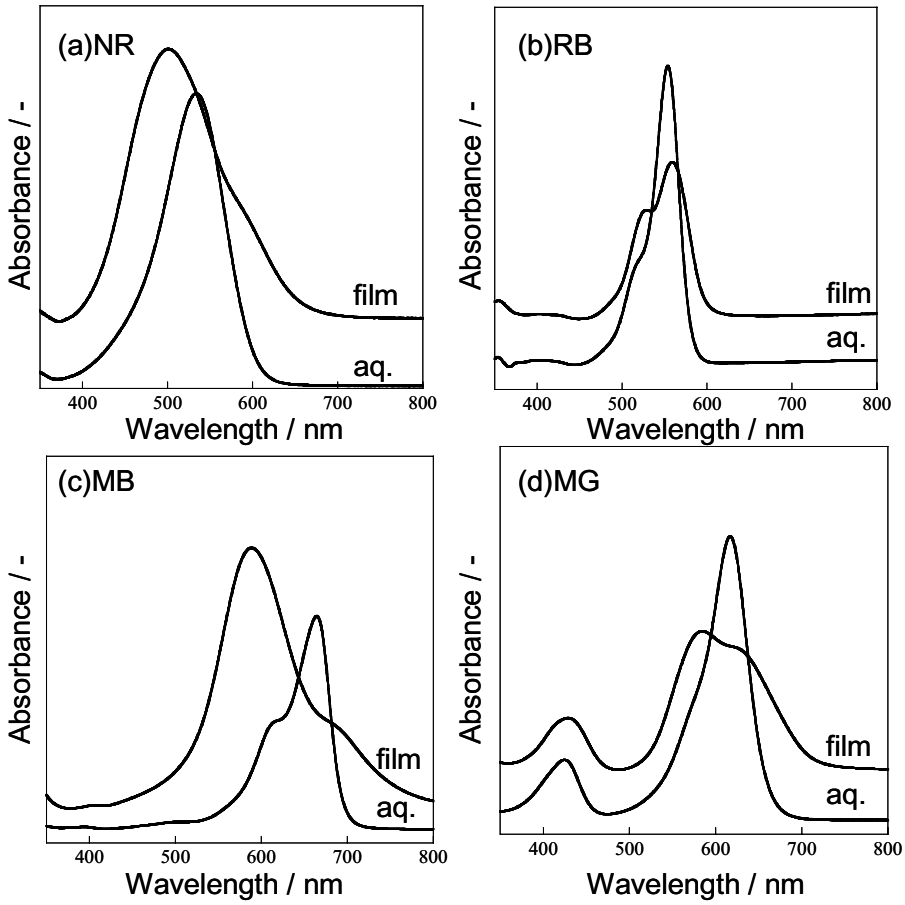

Figure 2. Absorption spectra of: (a) NR in aqueous solution and NR/SiO_2 film, (b) RB in aqueous solution and RB/SiO_2 film, (c) MB in aqueous solution and MB/SiO_2 film and (d) MG in aqueous solution and MG/SiO_2 film.

cross sign showing no colored or no deposition. In SiO_2 system, cationic dyes (MB, NR, RB and MG)/SiO_2 colored films were obtained whereas anionic dyes (EY, stilbazo, PCV and aluminon)/SiO_2 films were colorless. On the other hand, in TiO_2 and ZrO_2 systems, hybrid films of cationic MB and NR were obtained, however hybrid films of cationic RB and MG did not show any color. TiO_2 prepared by LPD process present a high degree of surface fluorination ($\equiv$Ti-F) (12,13). The fluoride chemisorption greatly reduces the positive surface charge on TiO_2 by replacing $\equiv$Ti-OH_2^+ by $\equiv$Ti-F species (14). Due to the negative surface charge on SiO_2, TiO_2 and ZrO_2, hybrid films of cationic dyes were formed. In SiO_2 system, colored hybrid films of cationic RB and MG could be fabricated because the electronegativity of Si is higher than that of Ti and Zr. As a result, fluorine adsorbs more easily onto Si than on Ti and Zr. In other words, the surface charge on SiO_2 is more negative than on TiO_2 and ZrO_2. Figure 2 shows the absorption spectra of free organic dyes in aqueous solution and organic dye/SiO_2 hybrid films. The shift of the absorption maximum upon incorporation is stronger in MB and NR than in RB and MG. This indicates that the interaction to SiO_2 is larger in MB and NR than in RB and MG. The cationic groups in RB and MG have weaker interaction due to steric hindrance of two ethyl groups (as illustrated in Scheme 1). Therefore, hybrid films of cationic RB and MG did not show any color in TiO_2 and ZrO_2 systems.

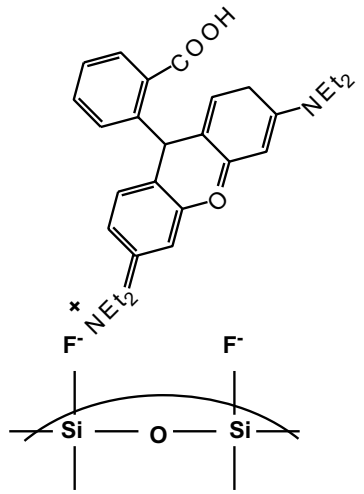

Scheme 1. Incorporation model of RB into SiO_2.

The formation of stilbazo/TiO_2 hybrid film as a function of the reaction time can be monitored by following the evolution of the absorption spectra as shown in Figure 3. The intensity of absorption increased as the reaction time passed. This result indicates that stilbazo not only adsorbed on TiO_2 surface, but also incorporated into the deposited film. Therefore, by using the LPD method, the organic compounds can be incorporated into various oxide films such as TiO_2, SiO_2 and ZrO_2.

Figure 4 shows Raman spectra of free MB in aqueous solution and MB/TiO_2 hybrid film. Characteristic peaks of MB at ~1600 cm^{-1} (ring stretch) and

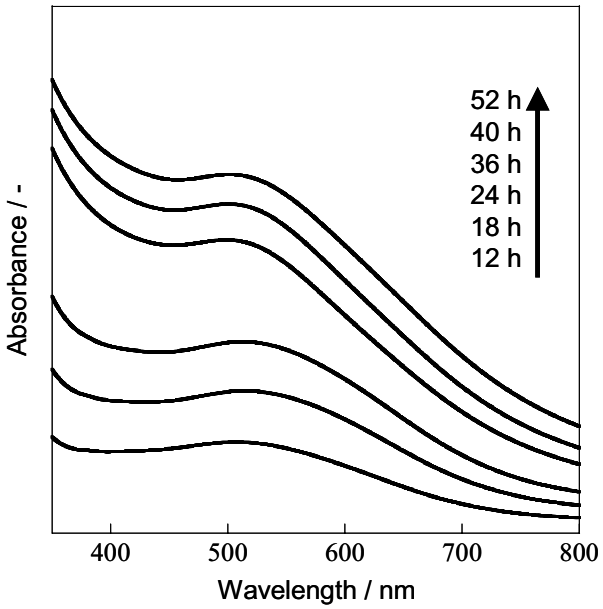

Figure 3. Absorption spectra of stilbazo/TiO_2 film as a function of the reaction time.

~1390 cm^{-1} (C–N symmetric stretch) appear in the MB/TiO_2 hybrid film. CN ring vibration shifted toward lower wavenumber from 1400 cm^{-1} to 1390 cm^{-1} upon incorporation. This shift indicates an interaction of the MB with TiO_2. It is thought therefore, that the electrostatic interaction between negative density charge at the TiO_2 fluorinated surface generated during the LPD process and the cationic MB ($Ti\text{-}F^{\delta-}:::MB^{+}$) is responsible of MB incorporation (15).

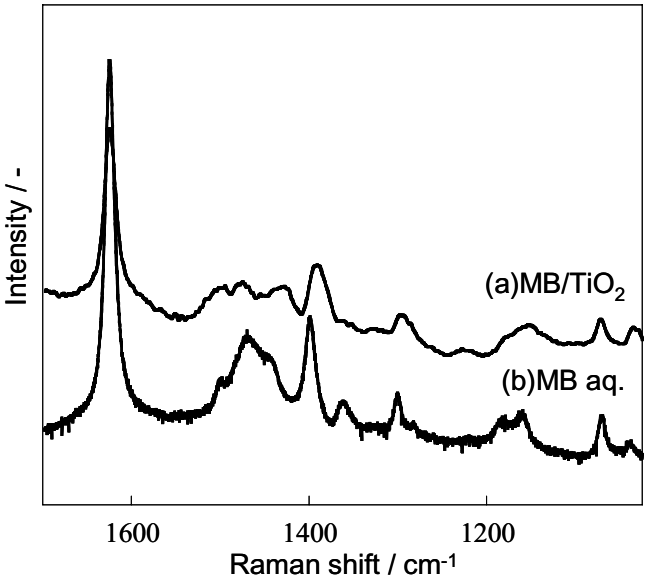

Figure 4. Raman spectra of: (a) MB/TiO_2 film and (b) MB in aqueous solution.

The XPS measurement was further employed to analyze fluorine of the surface of MB/TiO_2 hybrid film. The XPS technique provides a good tool for the study of interaction modes of MB with the TiO_2. Figure 5 shows the F 1s XPS spectra of MB/TiO_2 hybrid film and TiO_2 film. For TiO_2 film, only one F 1s peak at 684.3 eV was observed, which is attributed to F^- adsorbed on the surface of TiO_2. For MB/TiO_2 hybrid film, besides the peak at 684.2 eV, a new peak appeared at 685.7 eV. A positive shift of 1.5 eV in the F 1s binding energy of MB/TiO_2 hybrid film with respect to TiO_2 demonstrates that the chemical environment of fluorine is markedly different between the two systems. Therefore, in MB/TiO_2 hybrid film, MB should interact with the surface F site through the CN ring (as illustrated in Scheme 2).

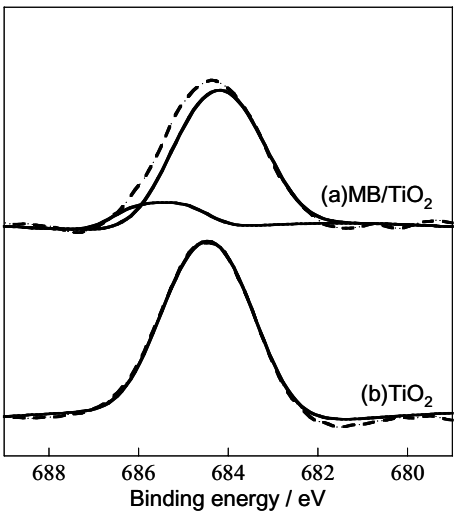

Figure 5. XPS spectra of F 1s:
(a) MB/TiO_2 film and (b) TiO_2 film.

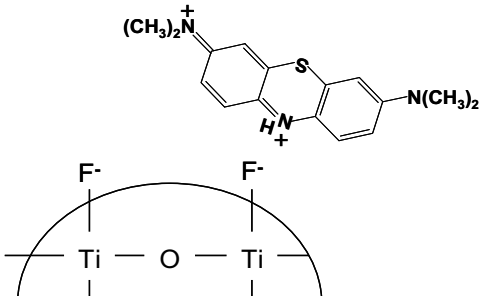

Scheme 2. Incorporation model of MB into TiO_2.

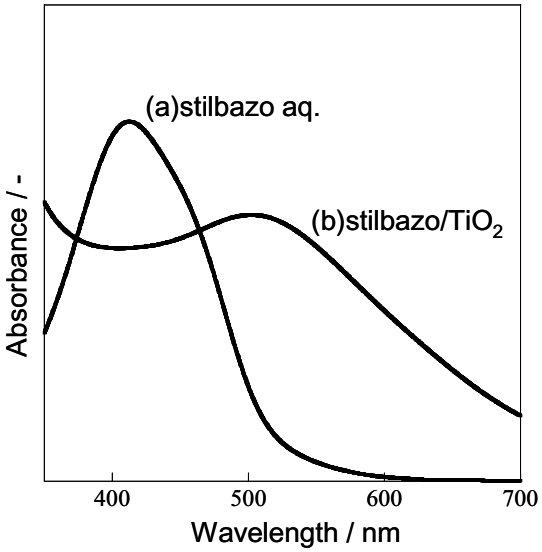

Figure 6. Absorption spectra of: (a) stilbazo in aqueous solution and (b) stilbazo/TiO_2 film.

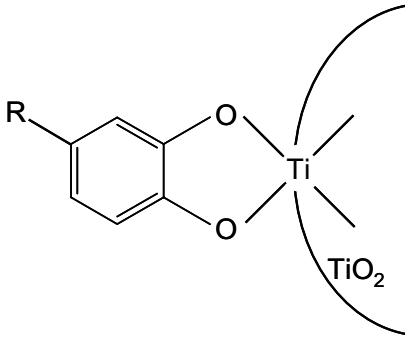

Scheme 3. Incorporation model of stilbazo into TiO_2.

Figure 6 shows the absorption spectra of free stilbazo in aqueous solution and stilbazo/TiO_2 hybrid film. For stilbazo/TiO_2 hybrid film, the absorption spectrum becomes broad and shifted to longer wavelength. This strong shift of the absorption maximum of about 90 nm from 410 to 500 nm upon incorporation indicates a very large electronic coupling between stilbazo and TiO_2, and the appearance of a new ligand-to-metal charge transfer absorption band. We assume that there is a linkage of stilbazo through the two chelating -OH groups of its catechol moiety to one surface Ti^{4+} ion with a bidentate linkage (as illustrated in Scheme 3). This is a favorable conformation of bond angles and distances for octahedrally coordinated surface of Ti atoms (16). It has been reported that TiO_2 can form a strong charge transfer complex with the catecholate dye molecule such as alizarin (17,18).

Figure 7 shows IR spectra of free aluminon in aqueous solution and aluminon/TiO_2 hybrid film. C-O stretching vibration shifted toward lower wavenumber from 1257 cm^{-1} to 1243 cm^{-1} upon incorporation. This shift indicates an interaction of the -OH group with TiO_2. The carboxylate bond could not be identified in aluminon/TiO_2 film. However, the degree of disassociation of the carboxyl group is higher than that of -OH group. Therefore, we assume that the carboxyl group bond to TiO_2, and there is a linkage of aluminon through the chelating -OH group and carboxyl group to one surface Ti^{4+} ion with a bidentate linkage as

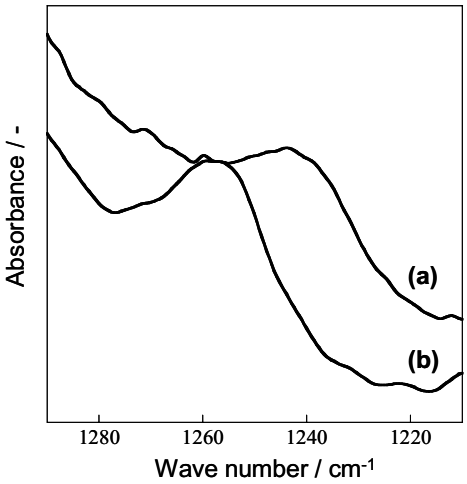

Figure 7. IR spectra of (a) aluminon/TiO_2 film and (b) aluminon in aqueous solution.

illustrated in Scheme 4 (19).

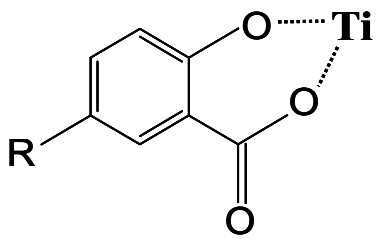

Scheme 4. Incorporation model of aluminon into TiO_2.

Characterization of organic dyes/metal oxide hybrid films

The density of dye molecules in the as-deposited stilbazo/TiO_2, PCV/TiO_2 and MB/TiO_2 films were calculated according to Lambert-Beer's Law from the absorbance of the dye at the absorption maximum (Table 2). The density of stilbazo and PCV was higher than that of MB, although molecular size of stilbazo and PCV is larger than that of MB. This indicates that the affinity of catecholate dye molecules (stilbazo and PCV) toward TiO_2 is better than that of MB.

Table 2. The density of organic dyes in TiO_2 film.

Sample	Density / Molecules・nm^{-3}
MB / TiO_2	0.074
PCV / TiO_2	0.973
stilbazo / TiO_2	0.124

The relationship between concentration of dye solution and the amount of deposited Ti was studied by ICP (Figure 8). By incorporating MB, there is no change in the amount of deposited Ti in TiO_2 and MB/TiO_2 films. However, the amount of deposited Ti decreased in the case of catecholate dye molecule as concentration of dye solution increases. Catechol dyes form chelate complex with TiF_6^{2-} in treatment solution. Therefore, catecholate dye molecules inhibit nuclear formation of TiO_2 and the amount of deposited Ti decreases.

Surface morphology of TiO_2 film and MB/TiO_2, stilbazo/TiO_2 and PCV/TiO_2 hybrid films deposited on glass slides were studied by SEM (Figure 9). TiO_2 and MB/TiO_2 film show dense and compact substrate coverage. The particle size is ca. 40 nm in the TiO_2 and MB/TiO_2 samples. On the other hand, stilbazo/TiO_2 and PCV/TiO_2 films show markedly uneven. The particle size is ca. 160 nm in stilbazo/TiO_2 sample and ca. 90 nm in the PCV/TiO_2 sample. The particle size

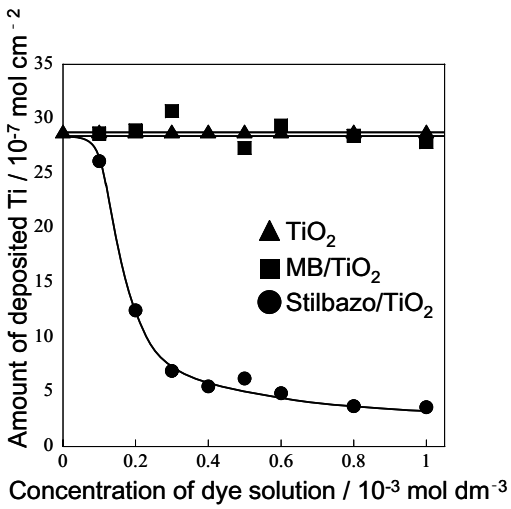

Figure 8. The relationship between concentration of dye solution and the amount of deposited Ti.

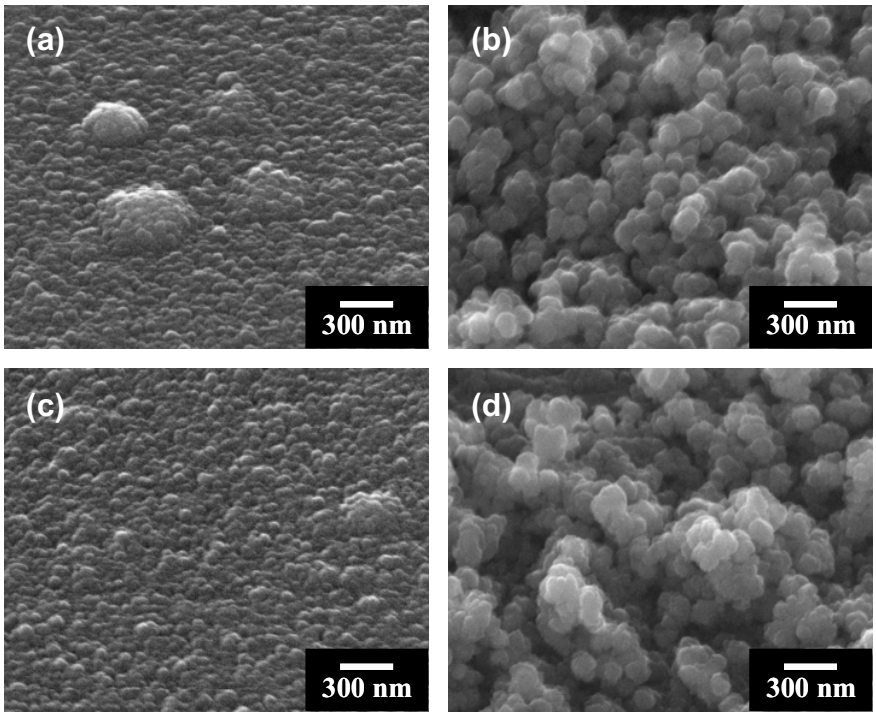

Figure 9. SEM images of: (a) TiO_2, (b) stilbazo/TiO_2, (c) MB/TiO_2 and (d) PCV/TiO_2 hybrid films.

in catechol dyes/TiO_2 films is considerably larger than in TiO_2 and MB/TiO_2 films. In treatment solution, catecholate dye molecules form a charge transfer complex with TiO_2 through the catechol moiety with a bidentate linkage. Therefore, catecholate dye molecules inhibit nuclear formation of TiO_2. As a result, TiO_2 particles in catechol dyes/TiO_2 samples grow larger. X-ray diffraction of TiO_2, MB/TiO_2, PCV/TiO_2 and stilbazo/TiO_2 films deposited on glass slides are shown in Figure 10. These diffraction peaks could be assigned to the anatase structure. It is well known that anatase is the TiO_2 phase usually favored by LPD, due to the presence of titanium strongly complexing ions such as the fluoride (13,20). Preferential *c* axis orientation has been reported previously both for TiO_2 films prepared by LPD, and has been attributed to the preferential adsorption of fluoride to planes parallel to this direction (21,(22). On the other hand, the intensity of (1 0 1) reflection of the anatase increased in the case of catechol

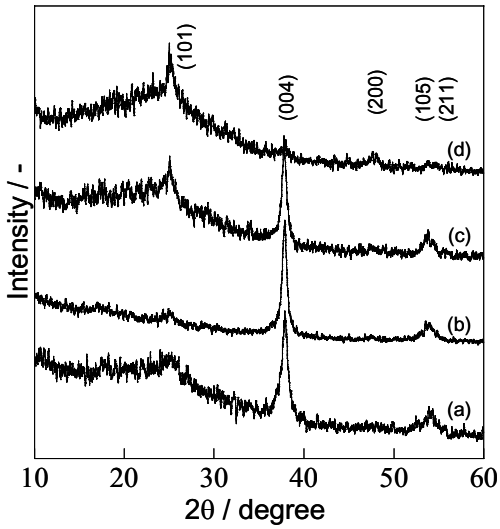

Figure 10. X-ray diffraction of: (a) TiO_2, (b) MB/TiO_2, (c) PCV/TiO_2 and (d) stilbazo/TiO_2 films.

dyes. It is caused by inhibition of nuclear formation of TiO_2.

Conclusion

The organic compound/metal oxide composite thin films have been successfully prepared by the LPD method. The development of LPD technique has open a way for the preparation of organic/inorganic hybrid materials.

Due to the negative surface charge on SiO_2, TiO_2 and ZrO_2, hybrid films of cationic MB and NR were fabricated. However, hybrid films of cationic RB and MG did not show any color in TiO_2 and ZrO_2 systems due to its steric hindrance. Catecholate dye molecules such as stilbazo and PCV have a linkage through the two chelating -OH groups of its catechol moiety to one surface Ti^{4+} ion with a bidentate linkage. It is assumed that there is a linkage of aluminon through the chelating -OH group and carboxyl group to one surface Ti^{4+} ion with a bidentate linkage.

The density of stilbazo and PCV in metal oxide film was higher than that of MB. This is because the affinity of catecholate dye molecules (stilbazo and PCV) toward TiO_2 is better than that of MB. There is no change in the amount of deposited Ti in TiO_2 and MB/TiO_2 films. However, the amount of deposited Ti decreased in the case of catecholate dye molecule. This implies that catechol dye forms chelate complex with TiF_6^{2-} in treatment solution and inhibits nuclear formation of TiO_2. The particle size of TiO_2 in stilbazo/TiO_2 and PCV/TiO_2 films is considerably larger than in TiO_2 and MB/TiO_2 samples. In treatment solution, catecholate dye molecules inhibit nuclear formation of TiO_2.

Acknowledgments

This work was supported by a Grant-in-Aid for Scientific Research (Project No. 19205029) from Ministry of Education, Culture, Sports, Science and Technology, Japan.

References

1. D. A. Loy, *Mater. Res. Bull.*, **26**, 364 (2001).
2. D. O'Hare in *Inorganic materials*; D. W. Bruce, D. O'Hare, Eds; John Wiley & Sons: Chichester, Brisbane, Toronto, Singapore, p.166 (1992).
3. G. A. Ozin, *Adv. Mater*., **4**, 612 (1992).
4. S. Y. Choi, M. Mamak, N. Coombs, N. Chopra and G. A. Ozin, *Nano Lett.*, **4**, 1231 (2004).
5. D. Gutiérrez-Tauste, I. Zumeta, E. Vigil, M. A. Hernández-Fenollosa, X. Domènech and J. A. Ayllón, *J. Photochem. Photobiol., A Chem.*, **175**, 165 (2005).
6. S. Deki, Y. Aoi, O. Hiroi and A. Kajinami, *Chem. Lett.*, **22**, 433 (1996).
7. S. Deki, Y. Aoi, Y. Miyake, A. Gotoh and A. Kajinami, *Mater. Res. Bull.*, **31**, 1399 (1996).
8. S. Deki, Y. Aoi and A. Kajinami, *J. Mater. Sci.*, **32**,4269 (1997).
9. S. Deki, Y. Aoi, J. Okibe, H. Yanagimoto, M. Mizuhata and A. Kajinami, *J. Mater. Chem.*, **7**, 1769 (1997).
10. L. Li, M. Mizuhata and S. Deki, *Appl. Surf. Sci.*, **239**, 292 (2005).

11. M. Tatemichi, M. Sakamoto, M. Mizuhata, S. Deki and T. Takeuchi, *J. Am. Chem. Soc.*, **129**, 10906 (2007).
12. J. G. Yu, H. G. Yu, B. Cheng, X. J. Zhao, J. C. Yu and W. K. Ho, *J. Phys. Chem. B*, **107**, 13871 (2004).
13. D. Gutiérrez-Tauste, X. Domènech, M. A. Hernández-Fenollosa and J. A. Ayllón, *J. Mater. Chem.*, **23**, 2249 (2006).
14. H. Park and W. Choi, *J. Phys. Chem. B*, **108**, 4086 (2004).
15. D. Gutiérrez-Tauste, X. Domènech, N. Casan-Pastor and J. A. Ayllón, *J. Photochem. Photobiol., A Chem.*, **187**, 45 (2007).
16. T. Rajh, J. M. Nedeljkovic, L. X. Chen, O. Poluektov, M. C. Thurnauer, *J. Phys. Chem., B*, **103**, 3515 (1999).
17. G. Ramakrishna, Sandeep Verma, D. Amilan Jose, D. Krishna Kumar, Amitava Das, Dipak K. Palit and Hirendra N.Ghosh, *J. Phys. Chem. B*, **110**, 9012 (2006).
18. R. Huber, S. Sporlein, J. E. Moser, M. Gratzel and J. Wachtveitl, *J. Phys. Chem. B*, **104**, 8995 (2000).
19. K. D. Dobson and A. J. McQuillan, *Spectrochim. Acta A*, **56**, 557 (2000).
20. H. Pizem, C. N. Sukenik, U. Sampathkumaran, A. K. McIlwain and M. R. De Guire, *Chem. Mater.*, **14**, 2476 (2002).
21. H. Pizem, O. Gershevitz, Y. Goffer, A. A. Frimer, C. N. Sukenik, U. Sampathkumaran, X. Milhet, A. McIlwain, M. R. De Guire, M. A. B. Meador and J. K. Sutter, *Chem. Mater.*, **17**, 3205 (2005).
22. A. M. Peiró, E. Vigil, J. Peral, C. Domingo, X. Domènech and J. A. Ayllón, *Thin Solid Films*, **411**, 185 (2002).